

# Early Holocene environment at a key location of the northwest boundary of the Asian summer monsoon: a synthesis on chronologies of Zhuye Lake, Northwest China

Yu LI\*, NaiAng WANG, ChengQi ZHANG, Yue WANG

Center for Hydrologic Cycle and Water Resources in Arid Region, College of Earth and Environmental Sciences, Lanzhou University, Lanzhou 730000, China

**Abstract:** The intensified monsoon increases summer rainfall and creates wet conditions in the Asian summer monsoon region during the early Holocene. Along with millennial-scale changes of the monsoon intensity, it is still unclear whether the boundary of the monsoon region changes according to monsoon variability. Investigations into the early Holocene environment in monsoon marginal zones are crucial for understanding the monsoon boundary changes. Zhuye Lake is located at the northwest edge of the Asian summer monsoon, the northern Qilian Mountains, which are less affected by modern summer monsoon water vapor. Previous studies have reached different conclusions regarding the early Holocene climatic and environmental changes based on different dating methods ( $^{14}\text{C}$  and OSL (optically stimulated luminescence)) and materials (shells, carbonate, pollen concentrates and bulk organic carbon). In this study, we synthesized 102  $^{14}\text{C}$  dates and 35 OSL dates from ten Holocene sedimentary sections and ten paleo-shorelines in the lake basin. A comparison between ages from different dating methods and materials generally shows that carbon reservoir effects are relatively slight in Zhuye Lake while the disordered chronologies are mainly related to the erosion processes and reworking effects. In addition, proxy data, including lithology, pollen, total organic carbon and carbonate, were collected from different sites of Zhuye Lake. According to the new synthesis, the early Holocene environment was relatively humid, associated with high runoff and lake water levels. The result indicates that the monsoon boundary moves to the north during the period of the intensified monsoon. A typical arid-area lake was formed during the mid-Holocene when carbonate accumulation and high organic matter contents were the main features of this period. The lake retreated strongly during the late Holocene, showing a drought trend. Overall, the lake evolution is generally consistent with the Holocene Asian summer monsoon change, showing the monsoon influence to monsoon marginal zones.

**Keywords:** the early Holocene;  $^{14}\text{C}$  dating; OSL dating; lacustrine sediments; Asian summer monsoon; monsoon marginal zones

**Citation:** Yu LI, NaiAng WANG, ChengQi ZHANG, Yue WANG. 2014. Early Holocene environment at a key location of the northwest boundary of the Asian summer monsoon: a synthesis on chronologies of Zhuye Lake, Northwest China. *Journal of Arid Land*, 6(5): 511–528. doi: 10.1007/s40333-014-0064-y

Holocene Asian summer monsoon evolution has been constructed by a variety of paleoclimate proxies in the past decade (An et al., 2000; He et al., 2004; Hong et al., 2005; Herzschuh, 2006; Chen et al., 2008; Wang et al., 2010). During the early Holocene, the Asian sum-

mer monsoon was strengthened by the increasing low-latitude solar insolation in the Northern Hemisphere, which has been widely confirmed by paleoclimate records in the typical monsoon domain (Fleitmann et al., 2003; Dykoski et al., 2005; Shen et al., 2005; Morrill

\*Corresponding author: Yu LI (E-mail: liyu@lzu.edu.cn)

Received 2013-09-24; revised 2013-10-25; accepted 2013-11-27

© Xinjiang Institute of Ecology and Geography, Chinese Academy of Sciences, Science Press and Springer-Verlag Berlin Heidelberg 2014

et al., 2006; Yancheva et al., 2007; Mischke et al., 2008; Cai et al., 2010; Wang et al., 2012). Afterwards, the intensity of monsoonal circulation declined in response to changes in solar insolation and a southward shift in the Intertropical Convergence Zone (Dykoski et al., 2005; Cai et al., 2010). Although much work has been devoted to the history of the Holocene Asian summer monsoon in the typical monsoon region, the changes in the northern boundary of the summer monsoon remain unclear. Li et al. (2012a) examined modern precipitation patterns (1960–2008) in the northwest margin of the Asian monsoon using field data of rainfall, water vapor transportation and geopotential height. According to their results, the Asian summer monsoon water vapor rarely reaches the northern Qilian Mountains, which are mostly affected by water vapor from the westerly winds (Li et al., 2012a). Whether the summer monsoon limit can move to the north during periods of strong monsoon, such as the early Holocene, is a key scientific issue. Early Holocene environmental records in Zhuye Lake are crucial for investigating variability of the summer monsoon limit. Furthermore, the Asian summer monsoon and the westerly winds interact in the mid-latitude regions (Zhang and Lin, 1992; Wang et al., 2005). Mid-latitude climates are dominated by the interaction of air masses, specifically cold air masses originating in high latitudes and warm air masses originating in the sub-tropical Highs (Aguado and Burt, 2004; Barry et al., 2004). As a result, the Zhuye Lake area, the terminal area of the Shiyang River, shares the cold winters, while the weather is relatively hot during summers (Zhang and Lin, 1992). The interaction between the Asian summer monsoon and the westerly winds plays a critical role in East Asia climate changes over several different time scales (Herzschuh, 2006; Chen et al., 2008). Precisely dated environmental records in Zhuye Lake can provide insights into the millennial-scale interaction between the monsoon and the westerly winds (Li et al., 2009a, b).

With regard to Holocene environmental changes in Zhuye Lake, previous studies reached different conclusions (Chen et al., 1999, 2001, 2003, 2006; Zhao et al., 2008; Li et al., 2009a, b; Long et al., 2010, 2012). Scientists have obtained Holocene lacustrine sediments from different sites of the lake basin. Holocene pollen, grain-size and geochemical records from the central part of the lake basin have shown the relatively

dry early Holocene and the mid-Holocene Climatic Optimum (Zhao et al., 2008; Li et al., 2009a, b; Long et al., 2010). However, lithology, pollen and geochemical records from the western lake basin indicated the humid early Holocene and a millennial-scale drought interval during the mid-Holocene (Chen et al., 2001, 2003, 2006). Both  $^{14}\text{C}$  and OSL dating methods have been used to date the paleo-shorelines in the northeast of the lake basin, but their results are different regarding the formation ages of the paleo-shorelines (Pachur et al., 1995; Zhang et al., 2004; Long et al., 2012). Generally, previous studies did not show the early Holocene environmental conditions clearly. The objective of the present paper is to study the early Holocene environmental change in Zhuye Lake by synthesizing Holocene  $^{14}\text{C}$  and OSL ages from lacustrine sediments and paleo-shorelines. In addition, proxy data from various sites of the lake basin, including lithology, pollen, total organic carbon and carbonate, were collected for a comparative research.

## 1 Study area

In the eastern Qilian Mountains and the eastern Hexi Corridor, the Shiyang River drainage area is roughly at the geographical coordinates of  $37^{\circ}02'–39^{\circ}17'\text{N}$ ,  $100^{\circ}57'–104^{\circ}57'\text{E}$ . The length of the drainage path is about 300 km and the total area is  $4.16 \times 10^4 \text{ km}^2$  (Fig. 1). Zhuye Lake, the terminal lake of the drainage area, is a tectonic rift basin, belonging to the Qilian Mountains piedmont fault basin (Chen and Qu, 1992; Fig. 2). The lake basin is about 65 km from east to west and about 20 km from south to north, while the lake basin center is approximately 1,290 m above sea level. The height difference between edge and central areas is about 30 m. In terms of geomorphic units, the Zhuye Lake area belongs to the alluvial plain in the lower reaches of the Shiyang River, where the annual average temperature is  $8–9^{\circ}\text{C}$  and average annual precipitation is 127.7 mm. There are 162 frost-free days per year, while the annual pan evaporation can reach 2,623 mm. The Quaternary unconsolidated lacustrine and alluvial sediments can reach up to a thickness of 300 m in the lake basin (Chen and Qu, 1992; Li et al., 2012b, c). At the northern foothills of the Qilian Mountains, the area is conducive to deposition of eolian sediments due to the blocking effect of the mountains. According to the geographical divisions of

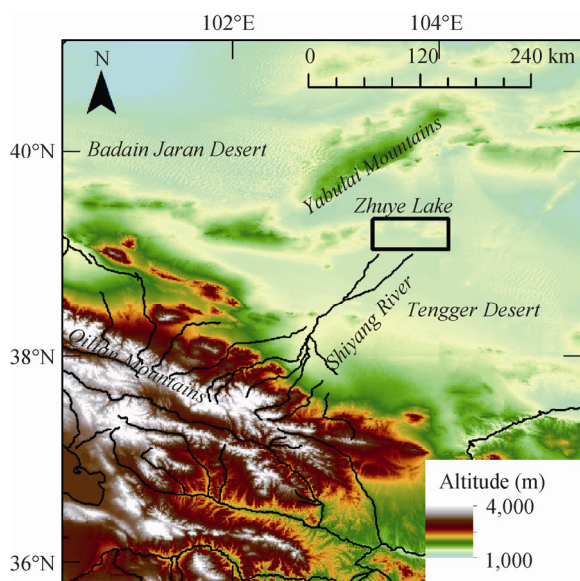


**Fig. 1** Map of the Shiyang River drainage area

China, the Zhuye Lake area is located in the typical arid region of Northwest China, where the modern climate is mainly controlled by the westerly winds and less affected by the Asian summer monsoon (Zhao, 1983; Wang et al., 2005; Li et al., 2012a). At the southern side of the Qilian Mountains, the northeastern margin of the Qinghai-Tibetan Plateau can still benefit from the Asian summer monsoon water vapor

transport, although the region does not belong to the typical monsoon region (Wang and Lin, 2002; Ding and Chan, 2005; Wang et al., 2005; Li et al., 2012a). However, water vapor transported by the monsoon can rarely reach the northern side of the Qilian Mountains (Li et al., 2012a). The Shiyang River drainage area can be divided into three climatic zones from south to north: (1) The alpine semi-arid area of the Qilian Mountains has an altitude of 2,000–5,000 m, annual precipitation of 300–600 mm and annual evaporation of 700–1,200 mm; (2) The cool and arid central plains have an altitude of 1,500–2,000 m, annual precipitation of 150–300 mm and annual evaporation of 1,300–2,000 mm; and (3) The northern warm and dry area has an altitude of 1,300–1,500 m, annual precipitation of less than 150 mm and annual evaporation of 2,000–2,600 mm (Chen and Qu, 1992). Zhuye Lake has dried up since the 1950s, as ever smaller amounts of water from the Shiyang River reached the area due to the increased irrigation in the upper reaches.

## 2 Materials and methods

During the Late Quaternary, a paleo-lake was formed in the Zhuye Lake area, while the lake level fluctuated

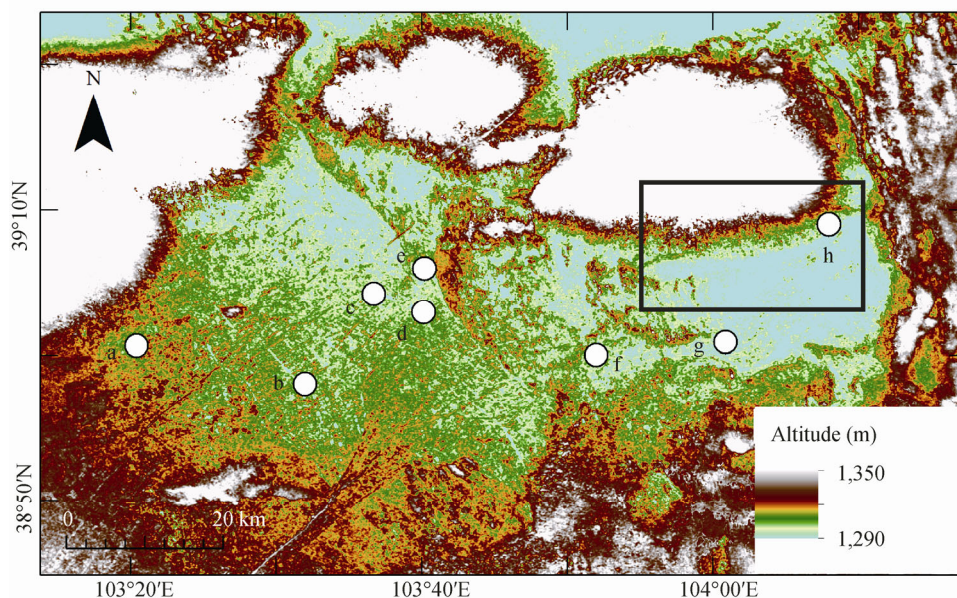


**Fig. 2** Topographic map of the Zhuye Lake basin. The white circles indicate locations of the ten Holocene sedimentary sections: (a) Sanjiaocheng, (b) XQ, (c) QTL-03, (d) QTH01 and QTH02, (e) Yiema, (f) SKJ, (g) Baijianhu and (h) BJ-S2 and JTL. The paleo-shorelines can be checked at the geographical coordinates of 37°05'–39°10'N, 103°55'–104°10'E on Google Earth.

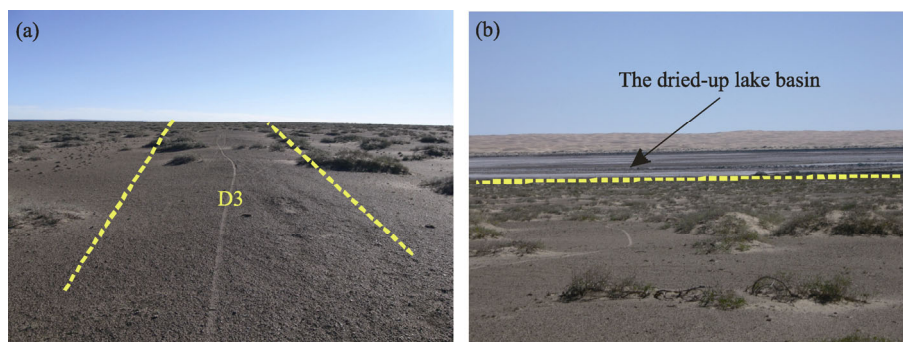


**Fig. 3** Photos of a typical paleo-shoreline and the dried-up lake basin in the northeast part of Zhuye Lake. (a) The D3 paleo-shoreline (39°08'44"N, 104°08'07"E); (b) The dried-up lake basin (39°08'50"N, 104°07'49"E).

frequently corresponding to orbital-scale climate change (Zhang et al., 2002); in modern times, lacustrine sediments and paleo-shorelines are widely distributed in the lake basin (Pachur et al., 1995; Fig. 3). Zhang et al. (2001, 2002, 2004) synthesized and updated the  $^{14}\text{C}$  dates of the Late Pleistocene paleo-shorelines and lacustrine sediments and found that the Late Pleistocene lake level reached its highest point during the MIS 3.

Lacustrine sediments in the Zhuye Lake basin are mainly characterized by grey, green or brown silt, with embedded sand layers indicating changes in hydrodynamic conditions, lake levels and sandstorm activity in adjacent areas. Some sedimentary layers are enriched with carbonate, mollusc shells or snails (Figs. 4–7). Ten Holocene sedimentary sections were investigated for  $^{14}\text{C}$ /OSL dating and analysis of proxy data, including pollen, grain-size and geochemical proxies (Table 1). QTH01 and BJ-S2 sections were dated by the OSL dating method; chronologies of other sections were established by the conventional or AMS  $^{14}\text{C}$  dating method (Tables 2 and 3). All OSL samples were obtained by hammering steel tubes (20 cm long cylinders with a diameter of 5 cm) into a freshly dug vertical section, next the tubes were covered and sealed with aluminum foil, and then wrapped using plastic bags and tape to avoid light exposure and moisture loss (Long et al., 2012). The water contents of the lacustrine sediments were measured in the field (still saturated). For each sample, the 38–63  $\mu\text{m}$  grains were separated by wet sieving, and then treated with fluorosilicic acid (38%) for about 2 weeks to corrode feldspars, followed by 10% HCl acid to remove fluoride

precipitates. The diffusion coefficient was determined using both the single aliquot regenerative-dose (SAR) protocol and a standardized growth curve (SGC) method (Long et al., 2010). The concentrations of uranium, thorium and potassium were measured by neutron activation analysis in China Institute of Atomic Energy in Beijing. OSL measurements were performed using an automated Risø TL/OSL-15 reader (Long et al., 2012). Various materials, such as bulk organic carbon, pollen concentrates, charcoal, carbonate, shells and snails, have been used for  $^{14}\text{C}$  dating (Table 2). The conventional  $^{14}\text{C}$  ages were mainly measured at the Radiocarbon Dating Laboratory of Lanzhou University and the AMS  $^{14}\text{C}$  ages were mostly measured by the Radiocarbon Dating Laboratory of Beijing University. For bulk organic matter, the pre-treatment of  $^{14}\text{C}$  dating was finished by the dating labs. The pre-treatment of pollen and charcoals  $^{14}\text{C}$  samples were described by Li et al. (2012c). The previously calibrated  $^{14}\text{C}$  ages were not used in this study, for different calibration methods can cause errors. All the  $^{14}\text{C}$  ages ( $^{14}\text{C}$  yr BP) were calibrated to calendar years (cal yr BP) using the software of Calib 6.11 (using IntCal'09; Reimer et al., 2009). Radiocarbon dating is the most commonly used method for establishing chronologies of lacustrine sediments; however,  $^{14}\text{C}$  ages of lacustrine sediments in arid regions are easily affected by carbon reservoirs that make the ages older than their true values (Morrill et al., 2006; Mischke et al., 2008; Li et al., 2009a, b). Terrestrial pollen concentrates, charcoal and macrofossils from lacustrine sediments were used as dating



**Fig. 4** Photos of typical Holocene sedimentary sections in Zhuye Lake. (a) JTL, (b) SKJ and (c) QTH02.

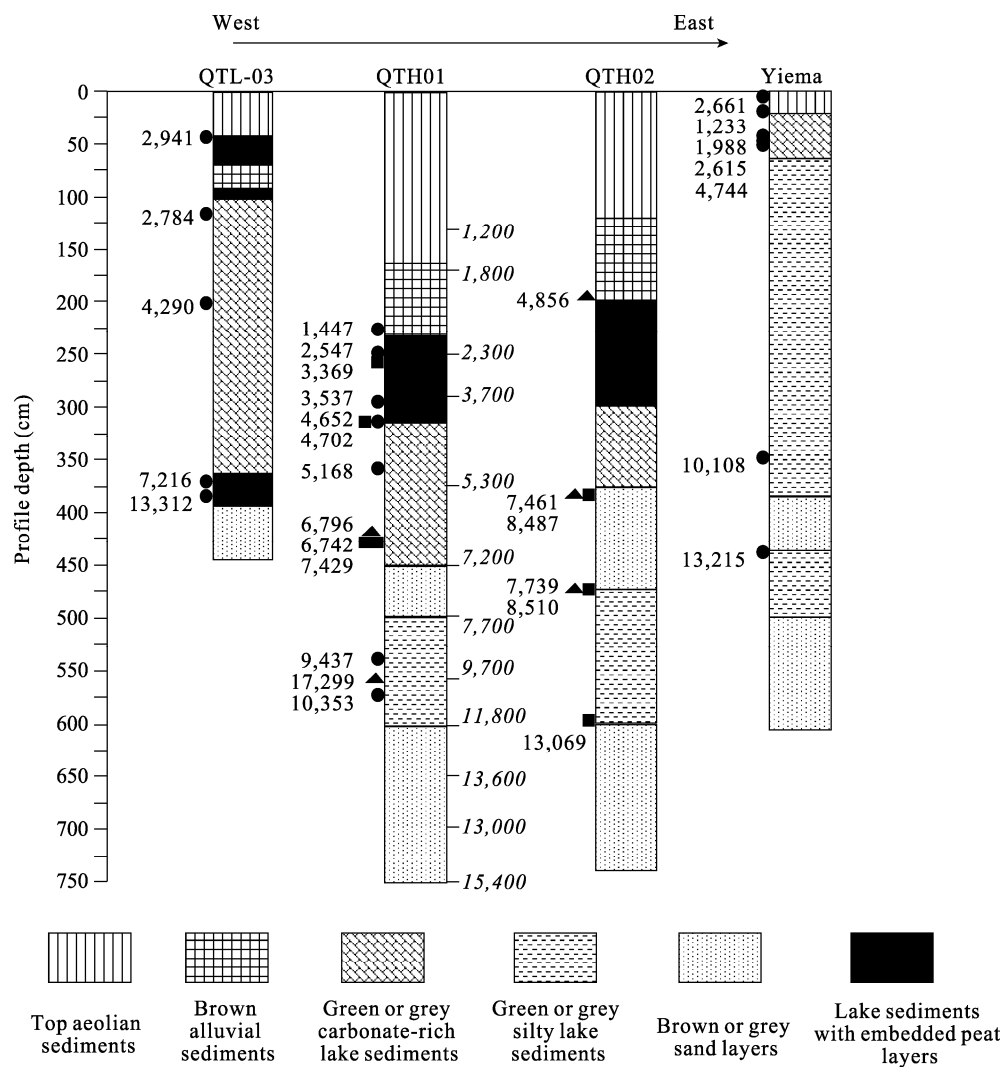


**Fig. 5** Lithology, the calibrated  $^{14}\text{C}$  dates (cal yr BP) and the OSL dates (yr BP) for QTH01, QTH02, QTL-03 and Yiema sections. Circles mean bulk organic carbon  $^{14}\text{C}$  dates; squares mean carbonate or shells  $^{14}\text{C}$  dates; triangles mean charcoals or pollen concentrates  $^{14}\text{C}$  dates; the OSL dates are shown in *italics*.

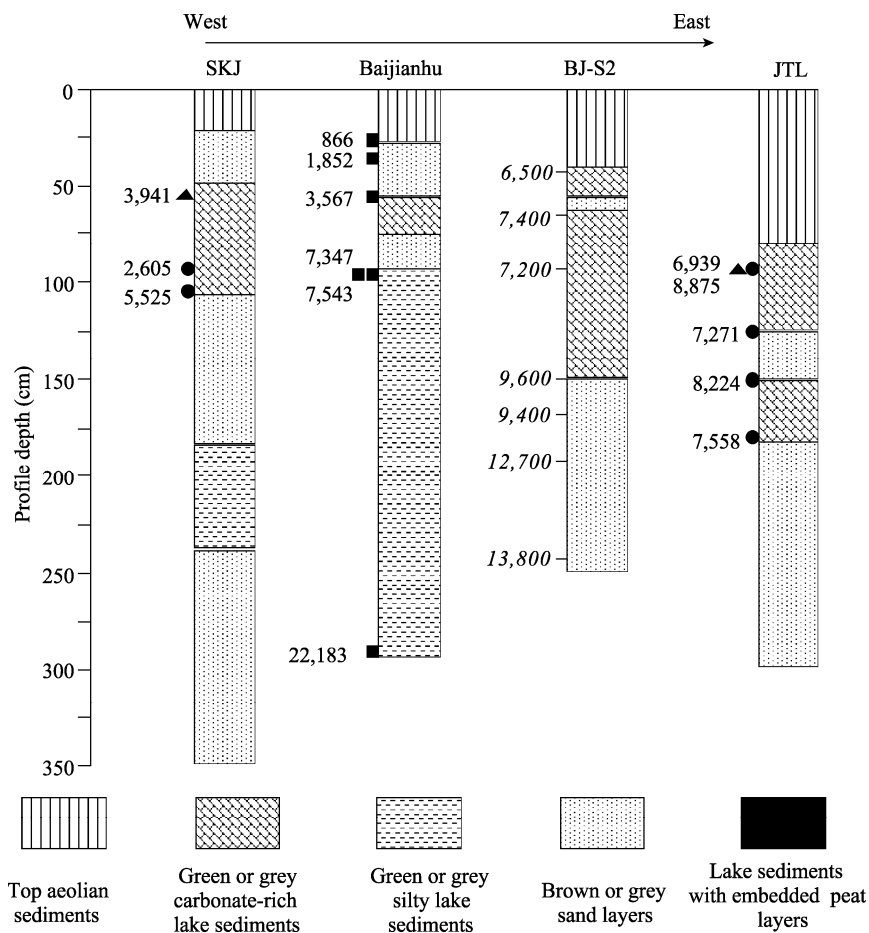


**Fig. 6** Lithology, the calibrated  $^{14}\text{C}$  dates (cal yr BP) and the OSL dates (yr BP) for Baijianhu, BJ-S2, JTL and SKJ sections. Circles mean bulk organic carbon  $^{14}\text{C}$  dates; squares mean carbonate or shells  $^{14}\text{C}$  dates; triangles mean charcoals or pollen concentrates  $^{14}\text{C}$  dates; the OSL dates are shown in italics.

**Table 1** List of sedimentary sections that were included in this study

Section	Coordinates	Elevation (m)	Profile depth (m)	References
Sanjiaocheng	39°00'N, 103°20'E	1,320	7.00	Chen et al. (2001, 2003, 2006)
XQ	38°58'N, 103°32'E	1,316	8.50	—
QTL-03	39°04'N, 103°36'E	1,302	3.80	Zhao et al. (2008)
QTH01	39°03'N, 103°40'E	1,309	7.50	Li et al. (2009a, b)
QTH02	39°03'N, 103°40'E	1,309	7.40	Li et al. (2009a, b)
Yiema	39°06'N, 103°40'E	1,300	6.00	Chen et al. (1999)
SKJ	39°00'N, 103°52'E	1,305	3.55	—
Baijianhu	39°01'N, 104°01'E	1,298	3.50	Pachur et al. (1995); Zhang et al. (2004)
BJ-S2	39°09'N, 104°08'E	1,308	2.40	Long et al. (2012)
JTL	39°09'N, 104°08'E	1,308	3.00	—

materials in order to avoid the carbon reservoir errors in Zhuye Lake (Chen et al., 1999, 2001, 2003; Li et al., 2009a, b). To provide the optimum chronological framework of lacustrine sediments, OSL dating was

also applied to date lacustrine sediments to overcome problems in  $^{14}\text{C}$  dating (Long et al., 2010, 2012). Palynological records and geochemical proxies (carbonate content and total organic carbon) from QTH01,

**Table 2**  $^{14}\text{C}$  ages from Baijianhu, Yima, QTL-03, Sanjiaocheng, QTH01, QTH02, XQ, JTL and SKJ sections

Section	Profile depth (m)	Dating materials	$^{14}\text{C}$ age (yr BP)	Calibrated $^{14}\text{C}$ age (2 $\sigma$ range) (cal yr BP)	Laboratory No./References
Baijianhu	0.26	Carbonate	970 $\pm$ 60	866 (738–977)	Zhang et al. (2004)
	0.34	Carbonate	1,910 $\pm$ 60	1,852 (1,714–1,988)	Zhang et al. (2004)
	0.57	Carbonate	3,320 $\pm$ 130	3,567 (3,263–3,890)	Zhang et al. (2004)
	0.92	Carbonate	6,420 $\pm$ 70	7,347 (7,177–7,460)	Zhang et al. (2004)
	0.92	Carbonate	6,670 $\pm$ 100	7543 (7,334–7,703)	Zhang et al. (2004)
	2.90	Carbonate	18,620 $\pm$ 325	22,183 (21,429–23,256)	Pachur et al. (1995)
Yima	0.00	Organic matter	2,580 $\pm$ 60	2,661 (2,461–2,842)	Chen et al. (1999)
	0.23	Organic matter	1,310 $\pm$ 60	1,233 (1,074–1,314)	Chen et al. (1999)
	0.40	Organic matter	2,030 $\pm$ 50	1,988 (1,882–2,120)	Chen et al. (1999)
	0.45	Organic matter	2,560 $\pm$ 80	2,615 (2,362–2,784)	Chen et al. (1999)
	0.53	Organic matter	4,230 $\pm$ 85	4,744 (4,523–5,030)	Chen et al. (1999)
	3.50	Organic matter	9,010 $\pm$ 160	10,108 (9,629–10,552)	Chen et al. (1999)
QTL-03	4.40	Organic matter	11,350 $\pm$ 274	13,215 (12,673–13,746)	Chen et al. (1999)
	0.40	Organic matter	2,835 $\pm$ 35	2,941 (2,857–3,063)	Zhao et al. (2008)
	1.18	Organic matter	2,675 $\pm$ 40	2,784 (2,744–2,853)	Zhao et al. (2008)
	2.06	Organic matter	3,860 $\pm$ 35	4,290 (4,156–4,412)	Zhao et al. (2008)
	3.74	Organic matter	6,285 $\pm$ 35	7,216 (7,159–7,289)	Zhao et al. (2008)
	3.80	Organic matter	11,445 $\pm$ 50	13,312 (13,180–13,428)	Zhao et al. (2008)
Sanjiaocheng	0.10	Organic matter	4,873 $\pm$ 130	5,614 (5,321–5,902)	Chen et al. (2001, 2003, 2006)
	0.90	Charcoal	2,450 $\pm$ 50	2,525 (2,356–2,708)	Chen et al. (2001, 2003, 2006)
	1.20	Charcoal	3,000 $\pm$ 95	3,180 (2,893–3,393)	Chen et al. (2001, 2003, 2006)
	1.45	Charcoal	3,110 $\pm$ 80	3,320 (3,077–3,548)	Chen et al. (2001, 2003, 2006)
	1.45	Organic matter	3,641 $\pm$ 95	3,967 (3,699–4,235)	Chen et al. (2001, 2003, 2006)
	1.65	Organic matter	4,010 $\pm$ 60	4,490 (4,294–4,804)	Chen et al. (2001, 2003, 2006)
	2.60	Organic matter	6,214 $\pm$ 75	7,109 (6,910–7,274)	Chen et al. (2001, 2003, 2006)
	3.00	Organic matter	7,670 $\pm$ 135	8,482 (8,181–8,969)	Chen et al. (2001, 2003, 2006)
	3.30	Organic matter	7,888 $\pm$ 140	8,746 (8,408–9,086)	Chen et al. (2001, 2003, 2006)
	4.70	Charcoal	9,840 $\pm$ 90	11,271 (10,882–11,692)	Chen et al. (2001, 2003, 2006)
	4.70	Organic matter	10,374 $\pm$ 260	12,118 (11,275–12,680)	Chen et al. (2001, 2003, 2006)
	5.25	Organic matter	14,340 $\pm$ 250	17,454 (16,869–18,023)	Chen et al. (2001, 2003, 2006)
	5.40	Pollen concentrates	15,900 $\pm$ 140	19,104 (18,798–19,412)	Chen et al. (2001, 2003, 2006)
	5.70	Organic matter	15,262 $\pm$ 450	18,420 (17,473–19,416)	Chen et al. (2001, 2003, 2006)
	2.25	Organic matter	1,550 $\pm$ 60	1,447 (1,316–1,551)	LUG96-44
	2.50	Organic matter	2,470 $\pm$ 90	2,547 (2,351–2,740)	LUG96-45
QTH01	2.62	Shells	3,140 $\pm$ 40	3,369 (3,263–3,448)	BA05223
	2.90	Organic matter	3,300 $\pm$ 90	3,537 (3,356–3,821)	LUG96-46
	3.15	Organic matter	4,130 $\pm$ 110	4,652 (4,298–4,953)	LUG96-47
	3.15	Shells	4,160 $\pm$ 40	4,702 (4,571–4,831)	BA05224
	3.60	Organic matter	4,530 $\pm$ 80	5,168 (4,881–5,449)	LUG96-48
	4.25	Carbonate	5,960 $\pm$ 65	6,796 (6,652–6,953)	LUG96-49
	4.25	Shells	5,920 $\pm$ 40	6,742 (6,658–6,854)	BA05225
	4.25	Pollen concentrates	6,510 $\pm$ 40	7,429 (7,322–7,494)	BA101234
	5.37	Organic matter	8,412 $\pm$ 62	9,437 (9,293–9,530)	LUG02-25
	5.61	Pollen concentrates	14,220 $\pm$ 50	17,299 (16,989–17,599)	BA101237
	5.72	Organic matter	9,183 $\pm$ 60	10,353 (10,234–10,502)	LUG02-23

To be continued

Continued

Section	Profile depth (m)	Dating materials	$^{14}\text{C}$ age (yr BP)	Calibrated $^{14}\text{C}$ age (2 $\sigma$ range) (cal yr BP)	Laboratory No./References
QTH02	1.99	Pollen concentrates	4,300 $\pm$ 25	4,856 (4,830–4,958)	BA101254
	3.88	Shells	6,550 $\pm$ 40	7,461 (7,344–7,563)	BA05222
	3.88	Pollen concentrates	7,705 $\pm$ 35	8,487 (8,413–8,575)	BA101256
	4.75	Shells	6,910 $\pm$ 40	7,739 (7,671–7,833)	BA05221
	4.75	Pollen concentrates	7735 $\pm$ 35	8,510 (8,432–8,587)	BA101257
XQ	5.91	Shells	11,175 $\pm$ 50	13,069 (12,875–13,241)	BA05218
	0.45	Organic matter	3,628 $\pm$ 58	3,946 (3,731–4,144)	Zhao et al. (2008)
	0.48	Pollen concentrates	5,855 $\pm$ 30	6,678 (6,567–6,745)	BA101249
	1.62	Organic matter	5,176 $\pm$ 68	5,937 (5,746–6,177)	Zhao et al. (2008)
	2.28	Organic matter	3,758 $\pm$ 65	4,126 (3,926–4,405)	Zhao et al. (2008)
	3.51	Organic matter	21,101 $\pm$ 220	25,220 (24,539–25,862)	Zhao et al. (2008)
	3.98	Pollen concentrates	22,380 $\pm$ 100	27,063 (26,301–27,716)	BA101248
	4.29	Organic matter	18,803 $\pm$ 207	22,431 (21,816–23,290)	Zhao et al. (2008)
	6.00	Organic matter	22,158 $\pm$ 189	26,618 (26,052–27,580)	Zhao et al. (2008)
	6.03	Pollen concentrates	21,000 $\pm$ 120	25,045 (24,575–25,510)	BA101247
	6.23	Organic matter	10,400 $\pm$ 80	12,275 (12,029–12,555)	Zhao et al. (2008)
	7.42	Organic matter	12,688 $\pm$ 117	14,992 (14,237–15,572)	Zhao et al. (2008)
	8.13	Pollen concentrates	15,360 $\pm$ 60	18,619 (18,499–18,792)	BA101246
	8.27	Organic matter	11,650 $\pm$ 110	13,512 (13,290–13,753)	Zhao et al. (2008)
JTL	0.98	Organic matter	6,071 $\pm$ 80	6,939 (6,744–7,162)	LUG-03-08
	1.00	Pollen concentrates	8,000 $\pm$ 40	8,875 (8,663–9,009)	BA101253
	1.29	Organic matter	6,350 $\pm$ 114	7,271 (6,987–7,475)	LUG-03-07
	1.50	Organic matter	7,410 $\pm$ 140	8,224 (7,952–8,454)	LUG-03-06
	1.81	Organic matter	6,688 $\pm$ 100	7,558 (7,419–7,732)	LUG-03-05
SKJ	0.58	Pollen concentrates	3,630 $\pm$ 25	3,941 (3,866–4,070)	BA101239
	0.93	Organic matter	2,541 $\pm$ 57	2,605 (2,366–2,759)	Zhao et al. (2008)
	1.14	Organic matter	4,808 $\pm$ 70	5,525 (5,324–5,659)	Zhao et al. (2008)

**Table 3** OSL ages for twelve samples at QTH01 section and seven samples at BJ-S2 section (Long et al., 2010, 2011, 2012). All the OSL dates were adjusted to AD 1950 to compare with calibrated  $^{14}\text{C}$  ages.

Section	Profile depth (m)	K (%)	Th ( $10^{-6}$ )	U ( $10^{-6}$ )	Dose rate (Gy/ka)	De (Gy)	OSL age (ka)
QTH01	1.30	1.93 $\pm$ 0.06	10.16 $\pm$ 0.35	2.50 $\pm$ 0.25	3.32 $\pm$ 0.24	4.10 $\pm$ 0.10	1.2 $\pm$ 0.1
	1.70	1.93 $\pm$ 0.06	6.04 $\pm$ 0.27	1.11 $\pm$ 0.18	2.65 $\pm$ 0.20	4.70 $\pm$ 0.09	1.8 $\pm$ 0.1
	2.50	0.58 $\pm$ 0.03	2.65 $\pm$ 0.16	11.19 $\pm$ 0.35	2.02 $\pm$ 0.16	4.70 $\pm$ 0.10	2.3 $\pm$ 0.2
	2.90	0.97 $\pm$ 0.04	4.34 $\pm$ 0.20	6.27 $\pm$ 0.27	1.76 $\pm$ 0.13	6.50 $\pm$ 0.20	3.7 $\pm$ 0.3
	3.75	0.32 $\pm$ 0.02	1.70 $\pm$ 0.14	4.08 $\pm$ 0.21	0.76 $\pm$ 0.07	4.10 $\pm$ 0.30	5.3 $\pm$ 0.6
	4.55	1.30 $\pm$ 0.05	2.93 $\pm$ 0.18	4.47 $\pm$ 0.23	1.63 $\pm$ 0.12	11.80 $\pm$ 0.50	7.2 $\pm$ 0.6
	4.95	0.97 $\pm$ 0.03	2.82 $\pm$ 0.17	8.10 $\pm$ 0.28	1.49 $\pm$ 0.12	11.50 $\pm$ 0.30	7.7 $\pm$ 0.7
	5.60	1.17 $\pm$ 0.04	5.48 $\pm$ 0.25	10.65 $\pm$ 0.35	2.21 $\pm$ 0.18	21.60 $\pm$ 0.50	9.7 $\pm$ 0.8
	6.00	1.46 $\pm$ 0.05	7.63 $\pm$ 0.27	7.74 $\pm$ 0.30	2.08 $\pm$ 0.16	24.50 $\pm$ 1.00	11.8 $\pm$ 1.0
	6.50	1.88 $\pm$ 0.06	7.13 $\pm$ 0.27	1.50 $\pm$ 0.21	1.87 $\pm$ 0.14	25.41 $\pm$ 0.41	13.6 $\pm$ 1.1
	7.00	1.97 $\pm$ 0.06	5.31 $\pm$ 0.24	1.27 $\pm$ 0.20	2.31 $\pm$ 0.19	30.26 $\pm$ 0.31	13.0 $\pm$ 1.1
	7.50	1.97 $\pm$ 0.06	4.42 $\pm$ 0.21	1.09 $\pm$ 0.20	2.40 $\pm$ 0.19	36.90 $\pm$ 0.37	15.4 $\pm$ 1.2
BJ-S2	0.30	1.70 $\pm$ 0.06	7.82 $\pm$ 0.26	2.96 $\pm$ 0.18	3.34 $\pm$ 0.19	21.85 $\pm$ 0.69	6.5 $\pm$ 0.4
	0.60	1.85 $\pm$ 0.09	6.72 $\pm$ 0.15	1.41 $\pm$ 0.11	3.02 $\pm$ 0.19	22.30 $\pm$ 0.40	7.4 $\pm$ 0.5
	0.90	1.93 $\pm$ 0.06	5.89 $\pm$ 0.24	1.66 $\pm$ 0.17	3.09 $\pm$ 0.18	22.30 $\pm$ 0.60	7.2 $\pm$ 0.5
	1.30	1.86 $\pm$ 0.06	5.76 $\pm$ 0.23	1.23 $\pm$ 0.16	2.90 $\pm$ 0.18	28.00 $\pm$ 0.50	9.6 $\pm$ 0.6
	1.60	1.77 $\pm$ 0.07	4.85 $\pm$ 0.21	1.06 $\pm$ 0.16	2.72 $\pm$ 0.17	25.50 $\pm$ 0.50	9.4 $\pm$ 0.6
	1.90	1.53 $\pm$ 0.06	6.26 $\pm$ 0.27	1.48 $\pm$ 0.16	2.67 $\pm$ 0.16	33.80 $\pm$ 0.20	12.7 $\pm$ 0.8
	2.40	1.75 $\pm$ 0.06	6.27 $\pm$ 0.27	1.69 $\pm$ 0.15	2.91 $\pm$ 0.18	40.10 $\pm$ 1.20	13.8 $\pm$ 0.9

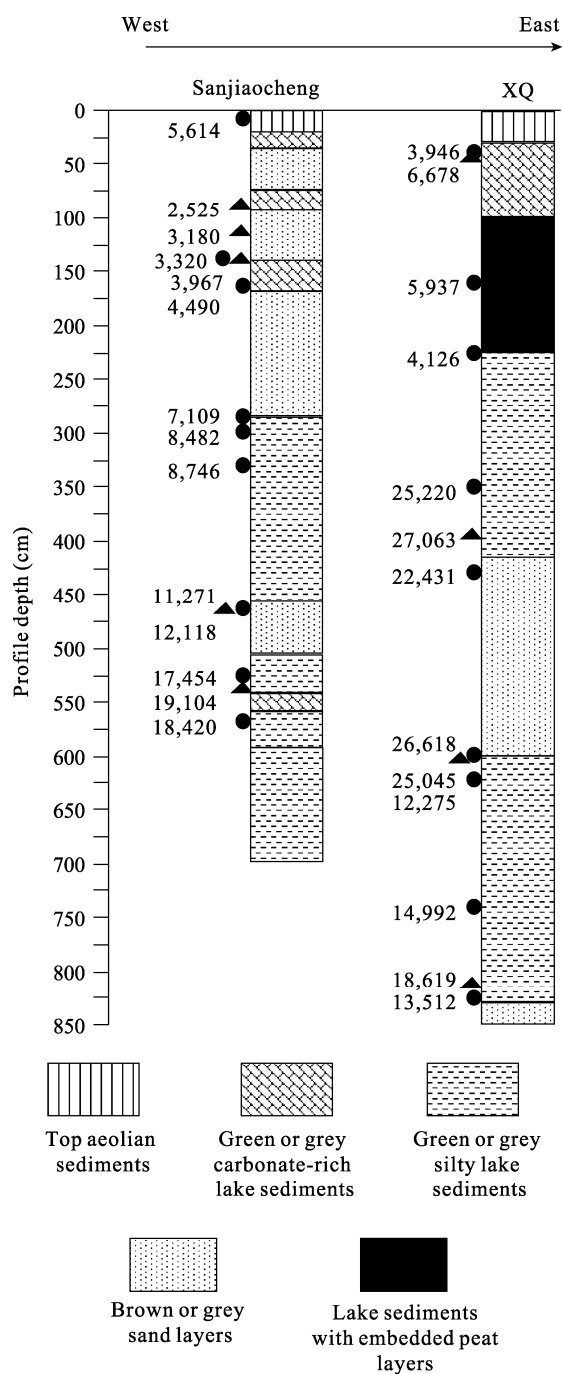


**Fig. 7** Lithology and the calibrated  $^{14}\text{C}$  dates (cal yr BP) for Sanjiaocheng and XQ sections. Circles mean bulk organic carbon  $^{14}\text{C}$  dates; squares mean carbonate or shells  $^{14}\text{C}$  dates; and triangles mean charcoals or pollen concentrates  $^{14}\text{C}$  dates.

QTH02, QTL-03 and Sanjiaocheng sections were collected for this study (Li et al., 2011). Figure 2 shows the topography of the lake basin and locations of the ten sedimentary sections. Figures 5–7 indicate lithologies and chronologies of QTH01, QTH02, QTL-03, Yiema,

Baijianhu, BJ-S2, SKJ, JTL, Sanjiaocheng and XQ sections. Photos of QTH02, SKJ and JTL sections are shown by Fig. 4.

Obvious paleo-shorelines are located in the north-east of the lake basin (Fig. 3). We used differential GPS and 1:50000 topography maps to determine elevations of those paleo-shorelines. Totally, nine paleo-shorelines were measured (Table 4). Pachur et al. (1995) have measured the locations and elevations of the paleo-shorelines, yet the results were restricted by the accuracy of GPS. It should be noted that the uppermost paleo-shoreline found by Pachur et al. (1995) was not studied, because its formation could be related to the topographic uplift and less correlated with the lake geomorphology according to our fieldwork. Figure 2 shows a remote sensing image for the north-east of the lake, where the paleo-shorelines were investigated, and Fig. 3 shows one of the paleo-shorelines (D3) and the modern dried-up lake basin. Since 1990s, these paleo-shorelines have been studied for their formation ages; however, there is still some controversy in terms of their ages. Tables 4 and 5 show the  $^{14}\text{C}$  and OSL ages from the paleo-shorelines (D1–D9).

### 3 Results

#### 3.1 Chronologies from different sedimentary sections

##### 3.1.1 QTH01, QTH02, QTL-03 and Yiema sections in the central part of the lake basin

QTH01 section is the best-dated sedimentary section in the lake basin. Thirteen  $^{14}\text{C}$  ages from bulk organic carbon, shells and pollen concentrates and twelve OSL ages have been obtained for QTH01 section (Fig. 5; Tables 2 and 3). Differences in ages from different dating materials and dating methods are relatively small. There are three OSL ages (11,800, 9,700 and 7,700 yr BP) and two  $^{14}\text{C}$  ages (10,353 and 9,437 cal yr BP) indicating the formation of green or grey silty sediments during the early Holocene. A sand layer, which was formed at around 7.5 cal kyr BP, was embedded between the early and mid-Holocene deposits, followed by carbonate enriched sediments of the mid-Holocene. QTH02 section is close to QTH01 section and their lithologies are similar to each other. Two ages from shells (13,069 and 7,739 cal yr BP)

**Table 4**  $^{14}\text{C}$  ages for samples of shells, snails and carbonate at nine paleo-shorelines (D1–D9) in the northeast part of Zhuye Lake

Paleo-shorelines	Coordinates	Elevation (m)	Dating materials	$^{14}\text{C}$ age (yr BP)	Calibrated $^{14}\text{C}$ age (2 $\sigma$ ) (cal yr BP)	Lab No./References
D <sub>1</sub>	39°08'46"N 104°07'57"E	1,310	Shells	32,520±840	37,220 (35,142–38,936)	Zhang et al. (2004)
			Shells	31,520±840	36,022 (34,596–38,365)	Zhang et al. (2004)
			Shells	31,360±1,240	35,967 (33,267–38,796)	Zhang et al. (2004)
			Shells	29,480±560	33,995 (32,637–35,089)	Zhang et al. (2004)
			Shells	26,430±980	30,948 (29,187–33,132)	Zhang et al. (2004)
			Shells	22,710±380	27,352 (26,239–28,264)	Zhang et al. (2004)
			Shells	22,480±590	27,057 (25,489–28,476)	Zhang et al. (2004)
			Shells	22,220±180	26,719 (26,154–27,611)	Zhang et al. (2004)
			Shells	33,500±1,085	38,275 (35,619–40,965)	Pachur et al. (1995)
			Shells	32,435±840	37,121 (35,120–38,859)	Pachur et al. (1995)
			Shells	32,270±1,236	36,978 (34,592–39,978)	Pachur et al. (1995)
			Shells	30,330±560	34,937 (33,644–36,316)	Pachur et al. (1995)
			Shells	27,200±975	31,759 (29,835–34,404)	Pachur et al. (1995)
			Shells	23,370±380	28,176 (26,978–29,177)	Pachur et al. (1995)
			Carbonate	23,130±590	27,829 (26,270–29,228)	Pachur et al. (1995)
			Carbonate	16,540±120	19,713 (19,427–20,060)	Pachur et al. (1995)
D <sub>2</sub>	39°08'42"N 104°08'01"E	1,308	Carbonate	12,817±142	15,319 (14,596–16,280)	Pachur et al. (1995)
			Snails	8,450±90	9,452 (9,142–9,581)	Zhang et al. (2004)
			Snails	5,965±114	6,810 (6,534–7,156)	LUG-03-07
D <sub>3</sub>	39°08'44"N 104°08'07"E	1,302	Snails	5,530±40	6,333 (6,279–6,404)	BA04212
			Snails	5,360±60	6,141 (5,996–6,281)	Zhang et al. (2004)
			Snails	5,100±70	5,827 (5,661–5,989)	Zhang et al. (2004)
D <sub>4</sub>	39°08'42"N 104°08'10"E	1,301	Snails	5,250±70	6,040 (5,900–6,263)	Pachur et al. (1995)
			Carbonate	5,510±60	6,312 (6,190–6,410)	Pachur et al. (1995)
			Carbonate	5,510±60	6,312 (6,190–6,410)	Pachur et al. (1995)
D <sub>5</sub>	39°08'37"N 104°08'12"E	1,300	—	—	—	—
D <sub>6</sub>	39°08'37"N 104°08'15"E	1,298	Snails	3,560±60	3,855 (3,690–4,069)	Zhang et al. (2004)
			Snails	3,660±55	3,988 (3,843–4,147)	Pachur et al. (1995)
D <sub>7</sub>	39°08'34"N 104°08'22"E	1,296	—	—	—	—
D <sub>8</sub>	39°08'33"N 104°08'25"E	1,295	Carbonate	1,860±60	1,795 (1,624–1,930)	Zhang et al. (2004)
			Carbonate	1,910±60	1,852 (1,714–1,988)	Pachur et al. (1995)
D <sub>9</sub>	39°08'32"N 104°08'26"E	1,294	Carbonate	1,405±60	1,320 (1,181–1,412)	Pachur et al. (1995)
			Carbonate	1,370±60	1,292 (1,175–1,386)	Zhang et al. (2004)

and one age from pollen concentrates (8,510 cal yr BP) indicate the Late Glacial and early Holocene deposition of sediments (Fig. 5; Table 2). Mid-to-late Holocene sedimentary sequences of QTH02 section are comparable to those of QTH01 section. One age (13,312 cal yr BP) at the bottom of QTL-03 section is relatively old; however, compared with QTH01 and QTH02 sections, QTL-03 section is not deep enough

to indicate the Late Glacial sediments. As a result, the relatively old age (13,312 cal yr BP) at QTL-03 section can be affected by the effects of  $^{14}\text{C}$  reservoir (Fig. 5; Table 2). In Yiema section, two ages of bulk organic carbon (13,215 and 10,108 cal yr BP) show that the Late Glacial and early to mid-Holocene sediments are relatively continuous on the millennial-scale and green or grey silty sediments are abundant during that period

**Table 5** OSL ages at ten paleo-shorelines (D1–D10) in the northeast part of Zhuye Lake (Long et al., 2012)

Paleo-shorelines	Elevation (m)	K (%)	Th ( $10^{-6}$ )	U ( $10^{-6}$ )	Dose rate (Gy/ka)	De (Gy)	OSL age (kyr BP)
D1	1,310	1.86±0.06	6.58±0.26	2.21±0.17	3.14±0.18	25.20±1.50	8.0±0.7
		1.78±0.06	7.25±0.27	2.83±0.18	3.27±0.18	25.10±1.40	7.7±0.6
		3.10±0.09	11.57±0.36	3.20±0.20	4.96±0.28	34.50±0.60	7.0±0.4
D2	1,308	2.03±0.06	3.56±0.23	1.04±0.15	2.74±0.17	13.50±0.40	4.9±0.3
		2.19±0.07	6.52±0.27	2.22±0.16	3.44±0.20	20.86±0.30	6.1±0.4
D3	1,302	1.92±0.06	11.63±0.28	2.04±0.13	3.55±0.19	13.20±0.20	3.7±0.2
D4	1,301	2.18±0.07	4.78±0.26	1.41±0.17	3.08±0.19	12.33±0.37	4.0±0.3
		1.77±0.06	7.58±0.30	2.73±0.19	3.27±0.18	11.59±0.30	3.5±0.2
D5	1,300	1.72±0.06	7.28±0.30	3.03±0.21	3.30±0.19	7.70±0.50	2.3±0.2
		2.14±0.07	6.05±0.26	1.93±0.17	3.28±0.19	7.90±0.20	2.4±0.2
D6	1,298	1.85±0.06	4.21±0.21	1.62±0.17	2.63±0.18	6.50±0.20	2.5±0.2
		1.87±0.06	6.17±0.25	2.17±0.19	3.16±0.18	7.30±0.10	2.3±0.1
D7	1,296	2.12±0.07	9.06±0.32	1.37±0.17	3.42±0.21	4.03±0.13	1.2±0.1
		1.96±0.06	6.60±0.28	1.51±0.16	3.12±0.19	6.82±0.07	2.2±0.1
D8	1,295	1.81±0.06	6.79±0.26	2.86±0.16	3.34±0.19	4.16±0.22	1.2±0.1
D9	1,294	2.43±0.08	8.36±0.32	2.03±0.16	3.85±0.23	4.30±0.05	1.1±0.1
D10	1,292	1.85±0.06	7.28±0.26	2.10±0.16	3.25±0.19	4.28±0.11	1.3±0.1
		1.86±0.06	6.17±0.27	1.83±0.16	3.11±0.18	4.64±0.16	1.5±0.1

(Fig. 5; Table 2). To sum up, the formation age of the Late Glacial and early Holocene lacustrine sediments begins at 13 cal kyr BP or even earlier in the central part of the lake basin. In some locations (QTH01 and QTH02 sections), the early Holocene sediments can be distinguished from the mid-Holocene deposits based upon their carbonate contents.

### 3.1.2 Baijianhu, SKJ, BJ-S2 and JTL sections in the eastern part of the lake basin

Baijianhu section in the eastern lake basin was dated by bulk carbonates and the results indicate that green or grey silty lacustrine sediments were continuously deposited between 22,183–7,543 cal yr BP on the millennial-scale (Fig. 6; Table 2). The mid-Holocene carbonate-enriched lacustrine sediments (7,347–3,567 cal yr BP) are comparable with those from the middle part of the lake basin. Seven OSL ages were obtained from BJ-S2 section, which indicate that the early to mid-Holocene carbonate-enriched lacustrine sediments are relatively continuous (Fig. 6; Table 3). JTL section is close to BJ-S2 section, and their lithologies and chronologies are similar to each other (Fig. 6; Table 2). The mid-Holocene carbonate-enriched lacustrine sediments were formed in the middle of the sec-

tion; however, the early and late Holocene lacustrine sediments cannot be traced. Lithology and chronology of SKJ section are relatively consistent with those from the center of the lake basin, since its location is close to the central part (Fig. 6; Table 2). The carbonate-enriched green or grey lacustrine sediments were deposited mainly during the mid-Holocene (5,525–3,941 cal yr BP). The early Holocene silty lacustrine sediments can be found in the deeper part of the section. Overall, the early Holocene green or grey silty lacustrine sediments were also formed in the eastern lake basin, which are more obvious in SKJ and Baijianhu sections.

### 3.1.3 Sanjiaocheng and XQ sections in the western part of the lake basin

In the western lake basin, fourteen  $^{14}\text{C}$  ages of bulk organic carbon, pollen concentrates and charcoal were obtained from Sanjiaocheng section, indicating a relatively well-dated sedimentary sequence since 18 cal kyr BP. As have been shown in Fig. 7 and Table 2, the Late Glacial and early Holocene green or grey silty lacustrine sediments were continuously deposited between 12,118–7,109 cal yr BP on the millennial-scale at the surface elevation of about 1,320 m, and the

mid-Holocene carbonate-enriched lacustrine sediments (about 225–100 cm) can be found in the upper part. The chronology from XQ section is relatively complicated, because  $^{14}\text{C}$  ages from the middle part of the section are older than those from the upper and lower parts. The Late Glacial lacustrine deposits have been formed since 13,512 cal yr BP according to the age from the bottom of XQ section, which are consistent with the beginning of the Late Glacial lacustrine sediments from QTH01, QTH02 and Yiema sections in the center of the lake basin (Figs. 5 and 7; Table 2). Generally, on the millennial-scale the green or grey silty lacustrine sediments were continuously deposited in the western lake basin during the Late Glacial and early Holocene and the beginning of the depositional processes was at around 13 cal kyr BP.

### 3.2 $^{14}\text{C}$ and OSL ages from paleo-shorelines

Table 4 shows the elevations and  $^{14}\text{C}$  ages of nine paleo-shorelines (D1–D9) in the northeast of Zhuye Lake. Seventeen  $^{14}\text{C}$  ages of carbonate and shells indicate that the D1 paleo-shoreline was formed between 37,220 and 15,319 cal yr BP. According to the ages, lake levels can reach the elevation during both the MIS 3 and the Late Glacial periods. The D2 paleo-shoreline was formed between 9,452 and 6,333 cal yr BP according to three  $^{14}\text{C}$  ages from snails, indicating the early to mid-Holocene high lake level. Shown by four  $^{14}\text{C}$  ages (5,827, 6,040, 6,141 and 6,312 cal yr BP) of carbonate and snails, the mid-Holocene paleo-shoreline (D3), at an elevation of 1,302 m asl, was relatively lower than the early to mid-Holocene one (D2). There are no  $^{14}\text{C}$  ages on paleo-shorelines D4 and D5, due to the lack of dating materials. Two ages from snails indicate the paleo-shoreline D6 was formed during the late Holocene (3,855 and 3,988 cal yr BP). Four ages from carbonate show that the paleo-shorelines D8 and D9 were formed between 1,852 and 1,292 cal yr BP. The earliest OSL age (8.0 kyr BP) is from the D1 paleo-shoreline and the other two OSL dates from the D1 paleo-shoreline are 7.7 and 7.0 kyr BP (Table 5). Two OSL ages (4.9 and 6.1 kyr BP) from the paleo-shoreline D2 indicate a relatively lower mid-Holocene lake level than the early Holocene one. The paleo-shorelines D3 and D4 were formed between

4.0–3.5 kyr BP on the basis of three OSL ages. Ten OSL ages show that paleo-shorelines D5–D10 were formed between 2.5–1.1 kyr BP, which are relatively consistent with the  $^{14}\text{C}$  ages. There are some differences between OSL and  $^{14}\text{C}$  ages at the D1 paleo-shoreline, which have been discussed by Long et al. (2012). Generally, the lake level in Zhuye Lake declined since the early Holocene based on these OSL and  $^{14}\text{C}$  ages, while high lake levels also appeared during the MIS 3 and the Late Glacial periods.

### 3.3 Proxy data

Carbonate, TOC and palynological records were obtained from four sedimentary sections (QTH01, QTH02, QTL-03 and Sanjiaocheng) of Zhuye Lake. Three of them (QTH01, QTH02 and QTL-03) are located in the center of the lake basin and the other is in the west (Chen et al., 2001, 2006; Zhao et al., 2008; Li et al., 2009a, b, 2011). Proxy data of the early Holocene (12.0–7.5 cal kyr BP) are characterized by high *Picea* pollen content and low contents of carbonate and total organic carbon. *Picea* pollen content was low during the mid-Holocene (7.5–3.0 cal kyr BP), but TOC and carbonate contents and pollen concentration were all high. Values of proxy data, including *Picea* pollen concentration, *Picea* pollen, total organic carbon (TOC) and carbonate contents, reached their lowest levels during the late Holocene (Fig. 8).

## 4 Discussion

### 4.1 Erosion processes and reworking effects in Zhuye Lake

On the northeast verge of the eastern lake basin, the early and late Holocene lacustrine deposits are missing at BJ-S2 and JTL sections. Erosion processes are always strong on the verge of a lake basin (Zhang et al., 2006; Long et al., 2012). Taking into account the locations of these two sections, the Late Glacial and early Holocene lacustrine deposition processes could be discontinuous because of strong hydrodynamic conditions and erosion processes. The missing late Holocene lacustrine sediments can be related to the declined lake level, since the study site can be higher than the lake water level. The differences between OSL and  $^{14}\text{C}$  ages from the paleo-shorelines can also be linked to the erosion processes and reworking

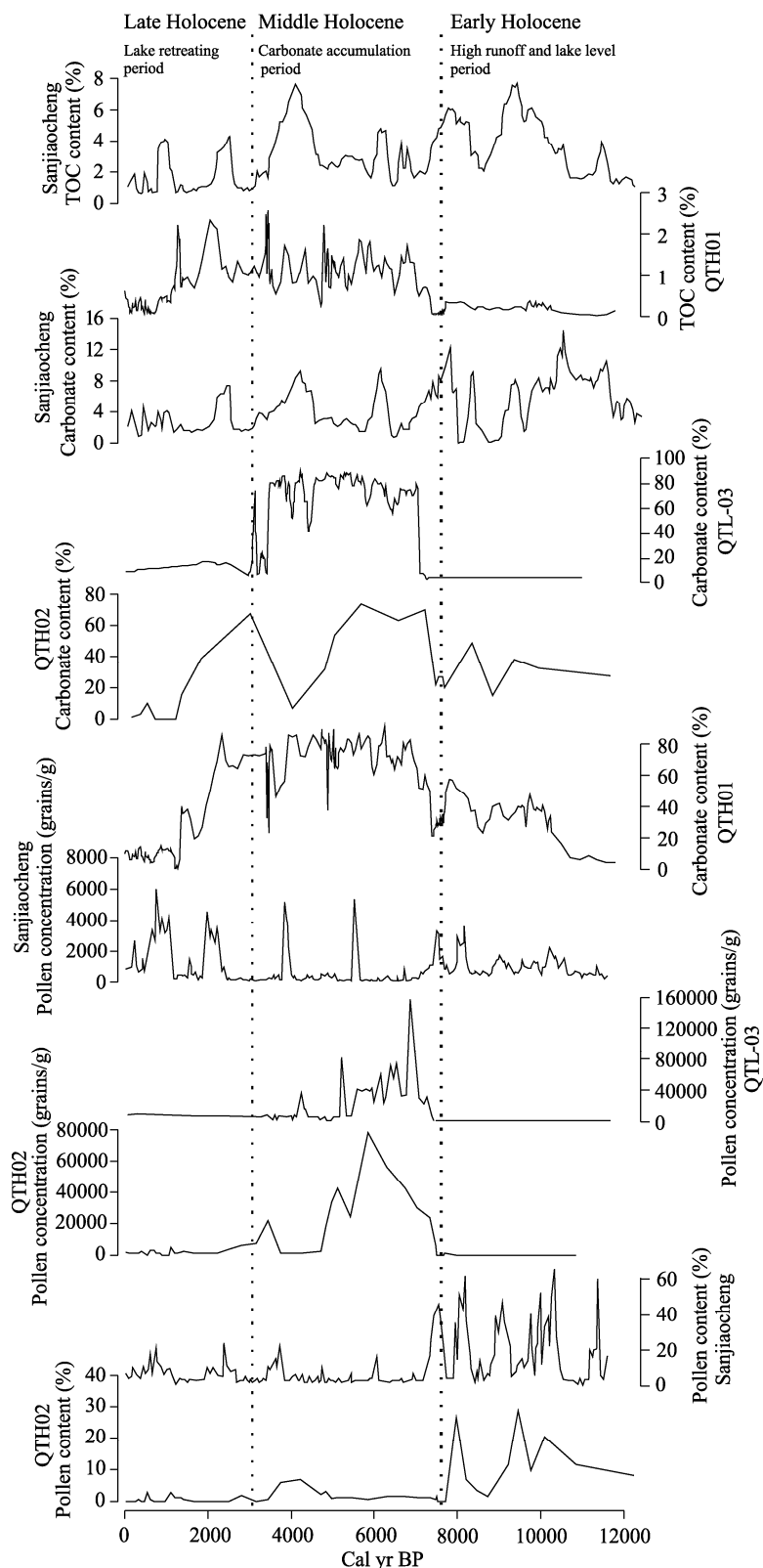


**Fig. 8** *Picea* pollen contents from Sanjiaocheng and QTH02 sections (Chen et al., 2006; Li et al., 2009a, b), pollen concentration from QTH02, QTL-03 and Sanjiaocheng sections (Chen et al., 2006; Zhao et al., 2008; Li et al., 2009a, b), contents of carbonate from QTH01, QTH02, QTL-03 and Sanjiaocheng sections (Chen et al., 2001; Zhao et al., 2008; Li et al., 2009a, b), and total organic carbon (TOC) contents from QTH01 and Sanjiaocheng sections (Chen et al., 2001; Li et al., 2009a, b) plotted against the calibrated  $^{14}\text{C}$  dates (cal yr BP)

effects. All three OSL ages from the D1 paleo-shoreline are very different from the  $^{14}\text{C}$  ages. In principle, there are some differences between the two dating methods. OSL dating measures the last time an object was exposed to sunlight;  $^{14}\text{C}$  dating measures residues, such as snails, shells or carbonate, on paleo-shorelines. Since the Late Pleistocene, the paleo-shorelines could have been influenced by erosion and reworking processes for many times, and the OSL ages can only record the latest formation of those paleo-shorelines. However, the  $^{14}\text{C}$  dates are based on preserved residues of paleo-shorelines, so that the  $^{14}\text{C}$  ages can be older than the OSL ages. As a result, lake levels can reach the elevation of the paleo-shoreline D1 during the MIS 3, the Late Glacial and the early Holocene periods according to the OSL and  $^{14}\text{C}$  dates, but the OSL ages only indicate the early Holocene paleo-shoreline due to the reworking effects. Meanwhile, the missing early Holocene lacustrine sediments at JTL and BJ-S2 sections near the paleo-shorelines can be correlated with the strong early Holocene reworking effects (Fig. 6; Tables 2 and 3). Due to the abundance of residues from the MIS3 and Late Glacial periods, lake water levels could be higher during those epochs. Generally speaking, the differences between OSL and  $^{14}\text{C}$  ages on the paleo-shorelines are mainly caused by the erosion processes and reworking effects. In the western lake basin, evidence of the reworking effects can be found in some sections based on a comparison between ages from different  $^{14}\text{C}$  dating materials. At XQ section,  $^{14}\text{C}$  ages from the middle part are much older than those from the lower part, while pollen concentrates, which have been recognized as a reliable dating material and are less affected by the carbon reservoir effects, were used for the dating. Besides, the pollen concentrates and bulk organic matter ages are similar to each other in the middle part. The disordered ages can be related to the reworking effects, because the relatively old sediments can be reworked to the study site and cause the old ages. Furthermore, the  $^{14}\text{C}$  ages of pollen concentrates are generally older than bulk organic matter ages at QTH01 and QTH02 sections. Pollen grains are small and light in weight, which are easily affected by the erosion processes and reworking effects. This can

be a reason for the relatively old ages (Li et al., 2012b, c). A comparison between ages from different dating methods and materials generally shows that the carbon reservoir effects are relatively slight in Zhuye Lake while the disordered chronologies are mainly related to the erosion processes and reworking effects. This viewpoint is consistent with previous studies on chronologies of Zhuye Lake (Chen et al., 2003, 2006; Li et al., 2009a, b; Long et al., 2010, 2011).

#### 4.2 An explanation of lithology and proxy data

The Late Glacial and early Holocene green or grey silty lacustrine sediments, for which depositions began at around 13 cal kyr BP and end at 7.5 cal kyr BP, are obvious in Zhuye Lake, according to lithologies and chronologies from SKJ, Baijianhu, QTH01, QTH02, Yiema, XQ and Sanjiaocheng sections. The mid-Holocene carbonate enriched lacustrine sediments can be found from various sites of the lake. Carbonate content is an important proxy to distinguish the early and mid-Holocene sediments. Peat, alluvial and eolian sediments were widely distributed in the lake basin during the late Holocene. Compared with the typical early to mid-Holocene lacustrine sediments, they indicate a decline in lake levels. *Picea* pollen, TOC and carbonate content can be used, in conjunction with lithology and chronology, to reconstruct the Late Glacial and Holocene lake evolution. *Picea* is a genus of coniferous trees, whose distribution is generally higher than 2,000 m asl in the Qilian Mountains (Huang, 1997). According to its modern distribution in East Asia, *Picea* forest cannot be distributed around the lake basin; therefore, it must have been transported by runoff from the mountains due to the lack of the ability to be transported by wind (Sugita, 1993; Huang, 1997; Liu et al., 1999; Zhu et al., 2003; Li et al., 2011). As a result, the high *Picea* pollen content in green or grey silty lacustrine sediments during the early Holocene can be correlated with high runoff. However, TOC and pollen concentration, which represent basin-wide primary productivity and vegetation intensity, and carbonate content were low during the early Holocene; on the contrary, their values were relatively high during the mid-Holocene. Basin-wide organic and inorganic sediments are transported by rivers to terminal lakes in inland drainage basins of Northwest

China. Precipitation, runoff and hydrodynamic conditions are generally strong during wet periods, when the depositional environment is not conducive for deposition and preservation of organic matter that is light in weight (Li et al., 2012b, c). This can be a reason for the low TOC and pollen concentration in green or grey silty lacustrine sediments. Meanwhile, adequate runoff can dilute carbonate concentration in lacustrine sediments, which leads to a low carbonate content. During the mid-Holocene, runoff decreased in the drainage basin and the hydrologic environment was relatively stable, so that organic matter and pollen can be preserved well in the terminal lake; therefore, both of their values were relatively high. A further retreat of the lake appeared during the late Holocene, indicating an intensive drought trend that can be implied by the low proxy data. All in all, high runoff and lake levels can be shown by *Picea* pollen and geochemical proxies from the early Holocene green or grey silty lacustrine sediments while the mid-Holocene depositional environment was conducive to the enrichment of carbonate, organic matter and pollen (Li et al., 2012b, c).

#### 4.3 A comparison between this research and previous studies

There are two views on the early to mid-Holocene environment in Zhuye Lake. The first view is that a wet climate prevailed during the Late Glacial and early Holocene (13.0–7.0 cal yr BP) periods and the mid-Holocene climate was relatively arid (7.0–5.0 cal yr BP), which were supported by lithologies, palynological and geochemical proxies from Yiema section in the center and Sanjiaocheng section in the west of the lake basin (Chen et al., 1999, 2001, 2003, 2006). The other view is that Holocene Climatic Optimum appeared during the mid-Holocene (7.5–4.5 cal yr BP), when lake level, vegetation intensity and moisture conditions reached their highest levels (Li et al., 2009a, b). Palynological and geochemical records (TOC and carbonate) from QTH01, QTH02 and QTL-03 sections in the central part of the lake basin provide evidence for the second view, which is also supported by lithology and chronology from BJ-S2 section in the east of the lake basin (Zhao et al., 2008; Li et al.,

2009a, b; Long et al., 2012). The main difference between the two viewpoints is whether the early Holocene or the mid-Holocene is wetter. Previous studies mostly focused on proxy data from a single section, which cannot be used to imply the depositional environment in the whole lake basin. Moreover, to understand proxies well, it is needed to consider a variety of factors. For example, pollen concentration and TOC are always used to imply basin-wide moisture conditions in arid regions, since moisture is the primary limiting factor for plant growth. Accordingly, the high pollen concentration and TOC during the mid-Holocene were used to imply an optimal environment (Zhao et al., 2008; Li et al., 2009a, b). Taking into account characteristics of these proxies, the high mid-Holocene TOC and pollen concentration can be related to stable hydrodynamic conditions and lake volume reduction that are conducive to enrichment of pollen and organic matter. On the contrary, the high early Holocene *Picea* pollen concentration can be seen as an indicator of high runoff and precipitation. Furthermore, the high early Holocene lake level is proved by widely distributed early Holocene green or grey silty lacustrine sediments and chronologies from paleo-shorelines. High carbonate content in the mid-Holocene sediments is another important evidence of the stable water environment and reduction in the volume of water. As a result, the difference of depositional environment between the early and mid-Holocene can be further distinguished by this study.

#### 4.4 Implications of this study

Different Holocene climate change patterns have been reported between the arid Central Asia and monsoonal regions (Fleitmann et al., 2003; Dykoski et al., 2005; Shen et al., 2005; Herzschuh, 2006; Yancheva et al., 2007; Chen et al., 2008; Mischke et al., 2008). Chen et al. (2008) synthesized the Holocene lake records in Central Asia, and confirmed the out-of-phase relationship between the effective moisture history in Central Asia and the Asian summer monsoon evolution. According to their results, a strong summer monsoon and humid climates prevailed in the Asian summer monsoon region during the early Holocene and the summer monsoon was weakened since the

mid-Holocene, which were mainly controlled by changes in low-latitude summer insolation. In contrast, the pattern of Holocene lake evolution in the arid Central Asia is mostly affected by the westerly winds that are associated with the North Atlantic sea-surface temperatures (SSTs), high-latitude air temperatures, and the amount and transport of water vapor (Herzschuh, 2006; Chen et al., 2008). The different changing patterns were also confirmed by paleoclimate models (Li and Morrill, 2010, 2013; Jin et al., 2012). The extension of the Asian summer monsoon was investigated in several studies (Morrill et al., 2003; Holmes et al., 2007), which mostly focused on the changing patterns of the Holocene Asian summer monsoon. Although a lot of work has been published for the Holocene climate change patterns in the monsoonal and arid Central Asia, there is no research indicating the movement of the northern boundary of Asian summer monsoon through an investigation of specific Holocene climatic records. Holocene climatic records from monsoon marginal zones have shown different environmental histories (Chen et al., 2003; Ma et al., 2003; Hartmann and Wünnemann, 2008). Dating errors, reworking effects and misunderstandings of proxies are main reasons for the different results (Zhang et al., 2006), and it is difficult to evaluate the accuracy of a record according to a single core or sedimentary section. Among these Holocene records, Zhuye Lake has attracted the attention of many scientists. Various sections and paleo-shorelines were investigated from different sites of the lake basin. This study, based on lithologies, chronologies and proxy data from ten sedimentary sections and ten paleo-shorelines, provided a reliable Holocene lake record in monsoon marginal zones, which proves that the monsoon northern boundary can move to the north corresponding to changes in the intensity of the Asian summer monsoon.

## 5 Conclusions

In this study, we synthesized 102  $^{14}\text{C}$  ages and 35 OSL ages from ten Holocene sedimentary sections and ten paleo-shorelines in Zhuye Lake, which is located in the monsoon marginal zone, a key area for studying the variability of the northern boundary of Asian

summer monsoon. The Late Glacial and early Holocene green or grey silty lacustrine sediments are widely distributed in different parts of the lake basin, which were deposited since 13.0 cal kyr BP. From 7.5 to 3.0 cal kyr BP, carbonate-enriched lacustrine sediments can be found in the lake basin, and the late Holocene was characterized by the shrink of the lake. A comparison between  $^{14}\text{C}$  and OSL ages of paleo-shorelines from the northeast of the lake clearly indicates that lake level began to decline since the early Holocene and a drought trend occurred during the late Holocene. Proxy data show that the early Holocene sediments are abundant with *Picea* pollen, which is an indicator of precipitation and runoff. High carbonate, TOC and pollen concentrations during the mid-Holocene are due to stable hydrodynamic conditions and reduction of lake water volume, indicating the retreat of the lake. Lacustrine sediments were replaced by eolian, alluvial or peat sediments in Zhuye Lake during the late Holocene, so that almost all proxies showed their lowest values. Our research shows that the high early Holocene runoff and lake levels in Zhuye Lake are consistent with the Asian summer monsoon records in typical monsoon areas, which are different from Holocene lake evolution in the arid Central Asia. Therefore, it further proves the impacts of the summer monsoon to monsoon marginal zones and the northern boundary of the Asian summer monsoon can move to the north during periods of strong monsoon. Further studies should focus on the millennial-scale climate mechanisms in the area; therefore, modern climate processes and climate models are needed for the investigation.

## Acknowledgements

This research was supported by the National Natural Science Foundation of China (41371009) and the Fundamental Research Fund for the Central Universities (Izujbky-2013-127). We thank the editor and reviewers for their constructive comments and suggestions that helped to improve this paper.

## References

- Aguado E, Burt J E. 2004. Understanding Weather and Climate (3<sup>rd</sup> ed.). New Jersey: Prentice Hall.
- An Z S, Porter S C, Kutzbach J E, et al. 2000. Asynchronous Holocene optimum of the East Asian monsoon. *Quaternary Science Reviews*, 19: 743–762.

- Barry R G, Chorley R J, Yokoi N J. 2004. *Atmosphere, Weather, and Climate* (8<sup>th</sup> ed.). London: Routledge.
- Cai Y J, Tan L C, Cheng H, et al. 2010. The variation of summer monsoon precipitation in central China since the last deglaciation. *Earth and Planetary Science Letters*, 291: 21–31.
- Chen C T A, Lan H C, Lou J Y, et al. 2003. The Dry Holocene megathermal in Inner Mongolia. *Palaeogeography, Palaeoclimatology, Palaeoecology*, 193: 181–200.
- Chen F H, Shi Q, Wang J M. 1999. Environmental changes documented by sedimentation of Lake Yiema in arid China since the Late Glaciation. *Journal of Paleolimnology*, 22: 159–169.
- Chen F H, Zhu Y, Li J J. 2001. Abrupt Holocene changes of the Asian monsoon at millennial-and centennial-scales: Evidence from lake sediment document in Minqin Basin, NW China. *Chinese Science Bulletin*, 46: 1942–1947.
- Chen F H, Wu W, Holmes J A, et al. 2003. A mid-Holocene drought interval as evidenced by lake desiccation in the Alashan Plateau, Inner Mongolia, China. *Chinese Science Bulletin*, 48: 1–10.
- Chen F H, Cheng B, Zhao Y, et al. 2006. Holocene environmental change inferred from a high-resolution pollen record, Lake Zhuyeze, arid China. *The Holocene*, 16: 675–684.
- Chen F H, Yu Z C, Yang M L, et al. 2008. Holocene moisture evolution in arid central Asia and its out-of-phase relationship with Asian monsoon history. *Quaternary Science Reviews*, 27: 351–364.
- Chen L H, Qu Y G. 1992. *Water-land Resources and Reasonable Development and Utilization in the Hexi Region*. Beijing: Science Press.
- Ding Y H, Chan J C L. 2005. The East Asian summer monsoon: an overview. *Meteorology and Atmospheric Physics*, 89: 117–142.
- Dykoski C A, Edwards R L, Cheng H, et al. 2005. A high-resolution, absolute-dated Holocene and deglacial Asian monsoon record from Dongge Cave, China. *Earth and Planetary Science Letters*, 233: 71–86.
- Fleitmann D, Burns S J, Mudelsee M, et al. 2003. Holocene forcing of the Indian monsoon recorded in a stalagmite from Southern Oman. *Science*, 300: 1737–1739.
- Hartmann K, Wünnemann B. 2008. Hydrological changes and Holocene climate variations in NW China, inferred from lake sediments of Juyanze palaeolake by factor analyses. *Quaternary International*, 194: 28–44.
- He Y, Theakstone W H, Zhang Z L, et al. 2004. Asynchronous Holocene climate change across China. *Quaternary Research*, 61: 52–63.
- Herzschuh U. 2006. Palaeo-moisture evolution in monsoonal Central Asia during the last 50,000 years. *Quaternary Science Reviews*, 25: 163–178.
- Holmes J A, Zhang J W, Chen F H, et al. 2007. Paleoclimatic implications of an 850-year oxygen-isotope record from the northern Tibetan Plateau. *Geophysical Research Letters*, 34: L23403.
- Hong Y T, Hong B, Lin Q H, et al. 2005. Inverse phase oscillations between the East Asian and Indian Ocean summer monsoons during the last 12000 years and paleo-El Niño. *Earth and Planetary Science Letters*, 231: 337–346.
- Huang D S. 1997. *Gansu Vegetation*. Lanzhou: Gansu Science and Technology Press.
- Jin L Y, Chen F H, Morrill C, et al. 2012. Causes of early Holocene desertification in arid central Asia. *Climate Dynamics*, 38: 1577–1591.
- Li Y, Wang N A, Cheng H Y, et al. 2009a. Holocene environmental change in the marginal area of the Asian monsoon: a record from Zhuye Lake, NW China. *Boreas*, 38: 349–361.
- Li Y, Wang N A, Morrill C, et al. 2009b. Environmental change implied by the relationship between pollen assemblages and grain-size in N.W. Chinese lake sediments since the Late Glacial. *Review of Palaeobotany and Palynology*, 154: 54–64.
- Li Y, Morrill C. 2010. Multiple factors causing Holocene lake-level change in monsoonal and arid central Asia as identified by model experiments. *Climate Dynamics*, 35: 1119–1132.
- Li Y, Wang N A, Li Z L, et al. 2011. Holocene palynological records and their responses to the controversies of climate system in the Shiyang River drainage basin. *Chinese Science Bulletin*, 56: 535–546.
- Li Y, Wang N A, Chen H B, et al. 2012a. Tracking millennial-scale climate change by analysis of the modern summer precipitation in the marginal regions of the Asian monsoon. *Journal of Asian Earth Sciences*, 58: 78–87.
- Li Y, Wang N A, Carrie M, et al. 2012b. Millennial-scale erosion rates in three inland drainage basins and their controlling factors since the Last Deglaciation, arid China. *Palaeogeography, Palaeoclimatology, Palaeoecology*, 365–366: 263–275.
- Li Y, Wang N A, Li Z L, et al. 2012c. Reworking effects in the Holocene Zhuye Lake sediments: A case study by pollen concentrates AMS <sup>14</sup>C dating. *Science China: Earth Sciences*, 55: 1669–1678.
- Li Y, Morrill C. 2013. Lake levels in Asia at the Last Glacial Maximum as indicators of hydrologic sensitivity to greenhouse gas concentrations. *Quaternary Science Reviews*, 60: 1–12.
- Liu H Y, Cui H T, Pott R, et al. 1999. The surface pollen of the woodland-steppe ecotone in southeastern Inner Mongolia, China. *Review of Palaeobotany and Palynology*, 105: 237–250.
- Long H, Lai Z P, Wang N A, et al. 2010. Holocene climate variations from Zhuyeze terminal lake records in East Asian monsoon margin in arid northern China. *Quaternary Research*, 74: 46–56.
- Long H, Lai Z P, Wang N A, et al. 2011. A combined luminescence and radiocarbon dating study of Holocene lacustrine sediments from arid northern China. *Quaternary Geochronology*, 6: 1–9.
- Long H, Lai Z P, Fuchs M, et al. 2012. Timing of Late Quaternary palaeolake evolution in Tengger Desert of northern China and its possible forcing mechanisms. *Global and Planetary Change*, 92–93: 119–129.
- Ma Y Z, Zhang H C, Pachur H J, et al. 2003. Late Glacial and Holocene vegetation history and paleoclimate of the Tengger Desert, north-western China. *Chinese Science Bulletin*, 48: 1457–1463.
- Mischke S, Kramer M, Zhang C J, et al. 2008. Reduced early Holocene moisture availability in the Bayan Har Mountains, northeastern Tibetan Plateau, inferred from a multi-proxy lake record. *Palaeogeography, Palaeoclimatology, Palaeoecology*, 267: 59–76.
- Morrill C, Overpeck J T, Cole J E. 2003. A synthesis of abrupt changes in the Asian summer monsoon since the last deglaciation. *The Holocene*, 13: 465–476.
- Morrill C, Overpeck J T, Cole J E, et al. 2006. Holocene variations in the

- Asian monsoon inferred from the geochemistry of lake sediments in central Tibet. *Quaternary Research*, 65: 232–243.
- Pachur H J, Wünnemann B, Zhang H C. 1995. Lake evolution in the Tengger Desert, northwestern China, during the last 40,000 years. *Quaternary Research*, 44: 171–180.
- Reimer P J, Baillie M G L, Bard E, et al. 2009. IntCal09 and Marine09 radiocarbon age calibration curves, 0–50,000 years cal BP. *Radiocarbon*, 51: 1111–1150.
- Shen J, Liu X Q, Wang S M, et al. 2005. Palaeoclimatic changes in the Qinghai Lake area during the last 18,000 years. *Quaternary International*, 136: 131–140.
- Sugita S. 1993. A modern pollen source area from an entire lake surface. *Quaternary Research*, 39: 239–244.
- Wang B, Lin H. 2002. Rainy season of the Asian–Pacific summer monsoon. *Journal of Climate*, 15: 386–396.
- WANG F N, LI B S, WANG J L, et al. 2012. Pleniglacial millennium-scale climate variations in northern China based on records from the Salawusu River Valley. *Journal of Arid Land*, 4(3): 231–240.
- Wang K L, Jiang H, Zhao H Y. 2005. Atmospheric water vapor transport from westerly and monsoon over the Northwest China. *Advances in Water Science*, 16: 432–438.
- Wang Y B, Liu X Q, Herzsuh U. 2010. Asynchronous evolution of the Indian and East Asian Summer Monsoon indicated by Holocene moisture patterns in monsoonal central Asia. *Earth-Science Reviews*, 103: 135–153.
- Yancheva G, Nowaczyk N R, Mingram J, et al. 2007. Influence of the intertropical convergence zone on the East Asian monsoon. *Nature*, 445: 74–77.
- Zhang H C, Ma Y Z, Li J J, et al. 2001. Palaeolake evolution and abrupt climate changes during last glacial period in NW China. *Geophysical Research Letters*, 28: 3203–3206.
- Zhang H C, Wünnemann B, Ma Y Z, et al. 2002. Lake level and climate changes between 42,000 and 18,000 C-14 yr BP in the Tengger Desert, Northwestern China. *Quaternary Research*, 58: 62–72.
- Zhang H C, Peng J L, Ma Y, et al. 2004. Late quaternary palaeolake levels in Tengger Desert, NW China. *Palaeogeography, Palaeoclimatology, Palaeoecology*, 211: 45–58.
- Zhang H C, Ming Q Z, Lei G L, et al. 2006. Dilemma of dating on lacustrine deposits in a hyperarid inland basin of NW China. *Radiocarbon*, 48: 219–226.
- Zhang J C, Lin Z G. 1992. *Climate of China*. New York: Wiley.
- Zhao S Q. 1983. A new scheme for comprehensive physical regionalization in China. *Acta Geographica Sinica*, 38: 1–10.
- Zhao Y, Yu Z, Chen F, et al. 2008. Holocene vegetation and climate change from a lake sediment record in the Tengger Sandy Desert, northwest China. *Journal of Arid Environments*, 72: 2054–2064.
- Zhu Y, Xie Y W, Cheng B, et al. 2003. Pollen transport in the Shiyang River drainage, arid China. *Chinese Science Bulletin*, 48: 1499–1506.